SIMULATION OF RESPIRATORY MECHANICS

RONALD W. JODAT, JAMES D. HORGAN, *and* RAMON L. LANGE
From the College of Engineering and the Medical School, Marquette University, Milwaukee, Wisconsin

ABSTRACT The dynamic relationship between respiratory muscle effort and the consequent changes in lung volume is investigated. A mathematical simulation based on the structures that form the connection between these two variables makes it possible to lump the contribution from all respiratory muscles into a single time-varying driving force. When this force is applied to the system model, the appropriate lung volume pattern results. The simulation results indicate the accuracy of the model and the validity of the lumped muscle force assumption. In addition, the system model adequately describes abnormal conditions such as decreased lung compliance and increased airway resistance. The results of this simulation suggest that the modeling technique is extremely useful in describing and analyzing complex respiratory system interactions.

INTRODUCTION

The mathematical description of ventilatory lung dynamics has been reported in the literature (6, 7, 9, 11, 13, 14, 17). More recently, the dynamics of the thorax and abdomen have been reported (1–5, 8, 18). The work of Agostoni is particularly useful in describing more completely the mechanics of the respiratory system. His work with thoracoabdominal mechanics provides necessary information about the respiratory actuating structures.

Fig. 1 shows the major respiratory control loop involving the chemical aspects. The respiratory actions controlled principally by carbon dioxide are effected through the mechanical dynamics. A complete simulation of the respiratory system must consider the mechanical and chemical dynamics united in their proper relationship. However, the emphasis in this paper is on the mechanical events involved in a single breath.

The respiratory control center (RCC) produces a neural discharge which results in a pattern of respiratory muscle activity sufficient to maintain proper ventilation. The movements of the respiratory muscles change the dimensions of the thoracic and abdominal cavities. These volumetric changes are then transmitted to the lungs. The purpose of this paper is to investigate the dynamic relationship between respiratory muscle effort and the variation in lung volume through the development of a model of the respiratory mechanics involved.

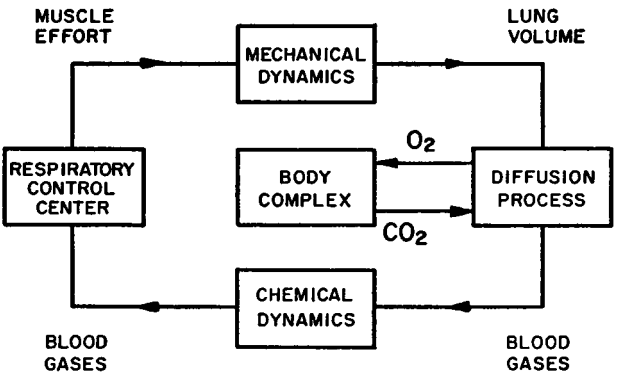

FIGURE 1 General block diagram of the respiratory system portraying it as a closed loop control system.

METHOD OF ANALYSIS

In this analysis, the response (lung volume) is known but the form of the excitation or driving force is not known. The solution may be approached in two steps:

(*a*) Formulation of a mathematical model of the system based on the knowledge of structure and function.

(*b*) Derivation of a driving function which when applied to the model will yield an appropriate response based on clinical experimental evidence.

System Model. The development of the system model is shown in Figs. 2 to 4. Fig. 2 is a general block diagram of the system to be simulated, which also suggests the

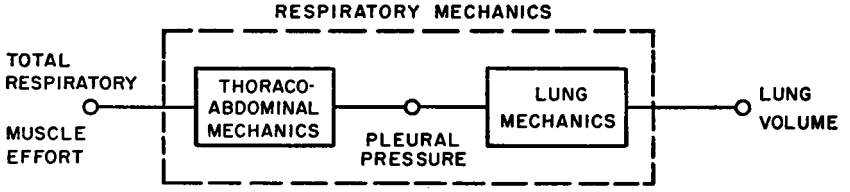

FIGURE 2 Subdivisions of respiratory mechanics.

approach to be used. The mechanics relating to total muscle force and lung volume consist of the thoracoabdominal and the lung portions. In the model these are related by the intermediate variable, pleural pressure. This variable was selected because it may be measured under many different circumstances, thereby providing a check on the model's accuracy.

A schematic of the system showing the structure and forces acting is contained in Fig. 3A. Fig. 3B is an equivalent representation in which the parameters of mass, compliance, and viscous resistance for each structure are shown.

The pleural cavity pressure varies during the respiratory cycle and in the model couples the thoracoabdominal to the lung dynamics. The pleural cavity in Fig. 3B is depicted as a compliant structure of small volume and represented by the three interconnected springs.

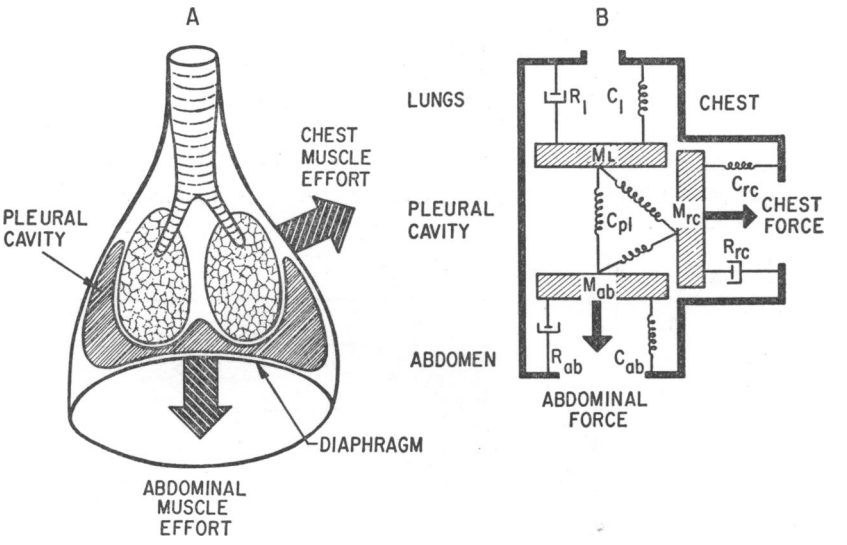

FIGURE 3 Respiratory structure: A. anatomical schematic; B. mechanical representation.

In the model, the pleural cavity compliance is assigned a value which can be made arbitrarily small along with the cavity volume. This is equivalent to representing it as a semirigid structure. Three other volumes appear in the model. V_l represents the lung volume.[1] V_{rc} and V_{ab} represent the changes in lung volume due to the action of the chest and abdominal forces. Abdominal and chest volumes are defined for the present purposes on a convenience basis rather than on an anatomical basis. These volumes account for the space occupied by the expanding lungs when the chest and diaphragm give way to initiate inspiration.

[1] *List of Symbols*

C_{ab}	abdominal compliance
C_{rc}	rib cage compliance
C_l	lung compliance
C_{pl}	pleural cavity compliance
FRC	functional reserve capacity
K_1	total muscle pressure parameter
K_2	total muscle pressure division constant
K_3	constant associated with functional relationship
M_{ab}	abdominal mass
M_l	lung mass
M_{rc}	rib cage mass
P_{ab}	abdominal pressure
$Patm$	atmospheric pressure
P_{FR}	pressure due to functional relationship
P_l	lung pressure
P_M	total muscle pressure
P_{MAX}	maximum Pmus (ab)
$P_{mus(ab)}$	abdominal muscle pressure
$P_{mus(rc)}$	rib cage muscle pressure
P_{pl}	pleural cavity pressure
P_{rc}	rib cage pressure
R_{ab}	abdominal damping
R_l	lung damping
R_{pl}	pleural cavity damping
R_{rc}	rib cage damping
V_{ab}	abdominal volume
V_l	lung volume
V_{pl}	pleural cavity volume
V_{rc}	rib cage volume

In addition to the above symbols, the convention of a dot over a symbol indicates a derivative with respect to time. Where possible the symbols follow the convention established by Mead (15).

The reference values for these volumes are: V_{l_0} = functional reserve capacity (FRC); V_{pl_0} = (static pleural pressure) × (compliance of pleural cavity); V_{rc_0} = zero; and V_{ab_0} = zero. The reference value V_{pl_0} was calculated by taking the product of the static pleural pressure (cm H_2O) and the assumed value of compliance (liters/cm H_2O). The reference values for V_{rc} and V_{ab} are zero.

The schematic of Fig. 3B can be translated into the working block diagram of Fig. 4 which shows the relationship between the driving forces (pressures) and the components of the changes in lung volume.

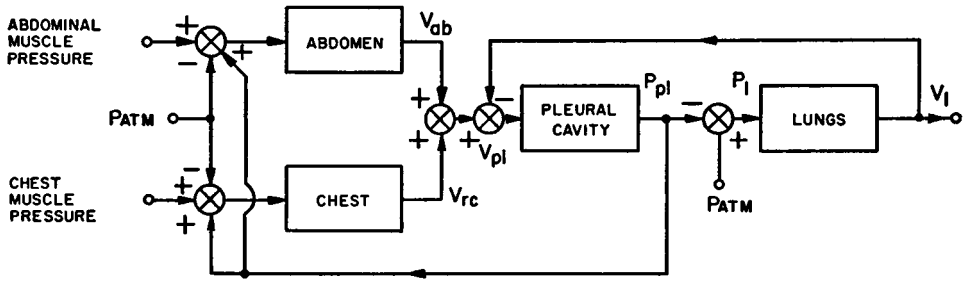

FIGURE 4 Double input block diagram of the respiratory system.

The complete block diagram is best understood by examining the manner in which the various volumes combine geometrically. Since the expanding chest and descending diaphragm create space that is filled by the enlarging lung and pleural volumes, we have

$$V_{ab} + V_{rc} = V_l + V_{pl}. \tag{1}$$

Rewritten, this equation as it is represented by the summing junction preceding the pleural cavity block in Fig. 4 becomes

$$V_{pl} = V_{ab} + V_{rc} - V_l. \tag{2}$$

The mathematical statements represented by the blocks may be developed by applying Newton's 2nd Law of Motion. In equations 3 to 5 the first terms represent inertial effects. The second terms represent viscous resistance forces. The third terms represent elastic forces. The quantities on the right-hand side of each equation represent the driving forces. By convention the sign is positive if it tends to expand the volume and negative if it compresses the volume of interest.

Lungs

$$M_l\ddot{V}_l + R_l\dot{V}_l + V_l/C_l = \text{PATM} - P_{pl} \tag{3}$$

Rib Cage

$$M_{rc}\ddot{V}_{rc} + R_{rc}\dot{V}_{rc} + V_{rc}/C_{rc} = P_{mus(rc)} + P_{pl} - \text{PATM} \tag{4}$$

Abdomen

$$M_{ab}\ddot{V}_{ab} + R_{ab}\dot{V}_{ab} + V_{ab}/C_{ab} = P_{mus(ab)} + P_{pl} - \text{PATM} \tag{5}$$

Equation 3 was fully developed by Mead (14), while equations 4 and 5 were developed by application of his technique. For simplification, the following assumptions are made:

(*a*) All mass terms were considered negligible when compared with the viscous and elastic terms.

(*b*) The pleural space is considered as a very stiff coupling among the lungs, chest, and abdomen. It is depicted as a very low compliance structure compared with the other compliances in the system.

(*c*) All parameters are considered linear and time invariant. The viscous resistance associated with the lung is mainly due to air flow.

(*d*) Sea level atmospheric pressure is the zero reference for all pressure measurements.

With these approximations and limitations the model equations become:

$$R_l \dot{V}_l + V_l/C_l = -P_{pl} \tag{6}$$

$$R_{rc} \dot{V}_{rc} + V_{rc}/C_{rc} = P_{mus(rc)} + P_{pl} \tag{7}$$

$$R_{ab} \dot{V}_{ab} + V_{ab}/C_{ab} = P_{mus(ab)} + P_{pl} \tag{8}$$

$$V_{pl} = V_{ab} + V_{rc} - V_l \tag{9}$$

$$P_{pl} = V_{pl}/C_{pl} \tag{10}$$

The sequence of equations 6 to 10 illustrate the iterative techniques used in solving the system model. Based on current values of the driving functions, the differential equations are solved for their respective volumes. These volumes are combined and a new value of pleural pressure is determined. The procedure is repeated with the new values of P_{pl} and the driving functions which represent the next time increment.

Driving Function. In order to compare the response of the system model with that of the prototype, the model must be subjected to a driving force. The actual forces are those produced by the various respiratory muscles. It is desirable to try to combine these individual forces into a single driving force. The measurable end result of total respiratory muscle effort is the production of a transdiaphragmatic pressure (TDP). This pressure difference across the diaphragm is equal to the abdominal minus the pleural pressure. The variations in the TDP are therefore proportionally related to the total driving force. Under the constraint that tidal volumes be restricted to their normal range (500 ml), it can be assumed that the total driving force would be similar in form. The TDP waveform is therefore termed the total muscle pressure curve.

Fig. 5 shows a representative curve of this pressure vs. time as determined from the data of Agostoni (1–3) plotted on a Campbell diagram. These plots display the varia-

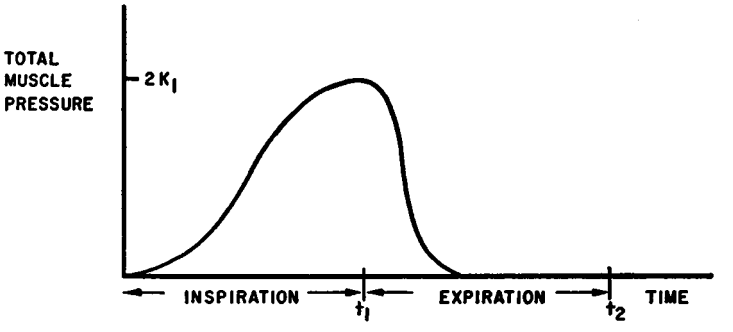

FIGURE 5 Muscle pressure driving function.

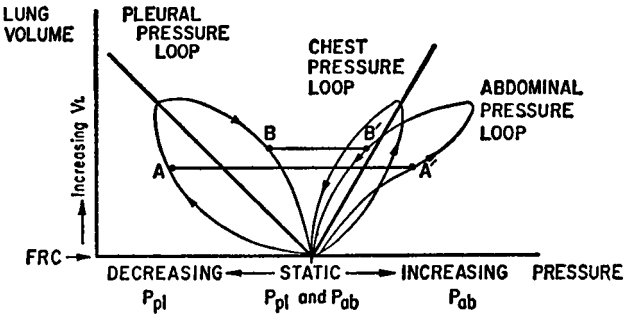

FIGURE 6 Representation of system pressures vs. lung volume. On this type of plot the point by point difference between the abdominal and pleural pressures is the transdiaphragmatic pressure. The arrows indicate the progression of time.

tion of pleural, abdominal, and chest pressure with respect to lung volume on a dynamic basis with the static characteristics also shown. An example of this type of plot is shown in Fig. 6.

The TDP or muscle pressure curve of Fig. 5 is represented in Fig. 6 by the pressure *A*—*A'* on inspiration and *B*—*B'* on expiration. An approximate fit of this curve is given by the following equation in which total muscle pressure (P_M) is the variable name used instead of TDP.

$$\begin{aligned} P_M &= K_1[1 - \cos(\alpha_1 t)]; \qquad 0 < t \leq t_1 \\ P_M &= K_1[1 + \cos(\alpha_2 t - \beta)]; \qquad t_1 < t \leq t_2 \end{aligned} \tag{11}$$

where:

$$\alpha_1 < \alpha_2$$

$$\beta = \alpha_1 t_1$$

The total muscle pressure (P_M) drives the rib cage and diaphragm. The portion acting on the rib cage is termed rib case muscle pressure $P_{mus(rc)}$ and that which activates the diaphragm is termed abdominal muscle pressure $P_{mus(ab)}$. The proportioning of P_M into $P_{mus(rc)}$ and $P_{mus(ab)}$ depends on whether the individual is predominantly a thoracic or a diaphragmatic breather. This can be stated mathematically as

$$\begin{aligned} P_{mus(rc)} &= K_2 P_M \\ P_{mus(ab)} &= [1 - K_2] P_M \end{aligned} \tag{12}$$

where K_2 characterized the breathing and has a value between 0 and 1. A typical value of K_2 would be 0.25 according to Agostoni (4, 5) who measured the contributions of the rib cage and abdomen-diaphragm to changes in lung volume.

The model also considers the interaction between the abdominal and chest cavities due to the rotation of the lower ribs about the vertebral-spinal axis. The initial muscle forces flattening the diaphragm also expand the lower portion of the rib cage. This coupling effect lasts only during the initial phase of inspiration and can be modeled by a functional

relationship block representing a saturation effect. The mathematical statements follow and their graphical interpretation is contained in Fig. 7.

Inspiration

$$\begin{aligned} P_{FR} &= P_{MA}; \qquad P_{MA} \leq K_3 \\ P_{FR} &= K_3; \qquad P_{MA} \geq K_3 \end{aligned} \tag{13}$$

Expiration

$$\begin{aligned} P_{FR} &= K_3 - P_{MAX} - P_{MA}; \qquad P_{MAX} - P_{MA} \leq K_3 \\ P_{FR} &= 0; \qquad P_{MAX} - P_{MA} \geq K_3 \end{aligned} \tag{14}$$

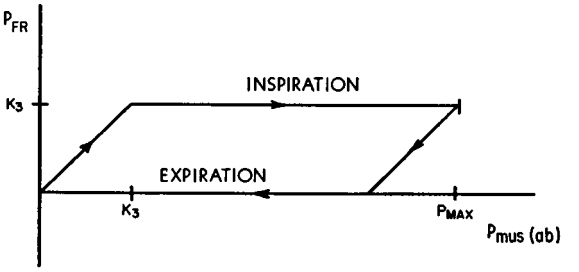

FIGURE 7 Abdominal-chest interaction.

In equations 13 and 14, P_{MAX} is the maximum value of $P_{mus(ab)}$ attained on inspiration, and K_3 is a constant which is a particular value of $P_{mus(ab)}$ above which the chest-abdomen interaction is ineffective. The block diagram including the muscle pressure division process is shown in Fig. 8.

The differential equations and their parameters that are symbolized by the blocks in Fig. 8 were programmed and solved on an IBM 1620 digital computer. The sources from which the parameter values were obtained are given in Table I. The flow resistance and compliance parameters for the abdominal structure were determined by experimentation on the model. The model solutions were found to be stable and the generated TDP quantitatively correct for the chosen abdominal parameters.

The above representation constitutes the mathematical simulation of the actual system.

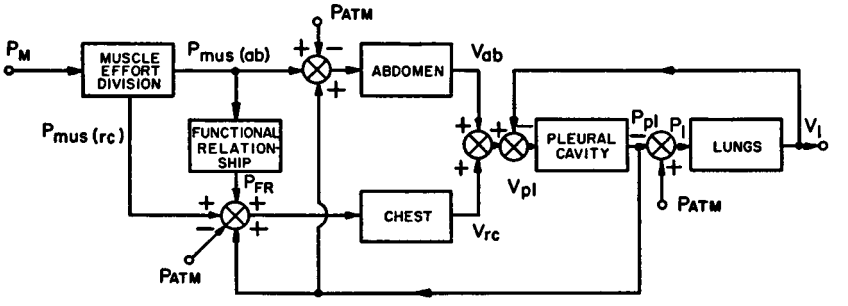

FIGURE 8 Single input block diagram of the respiratory system.

TABLE I

SIMULATION PARAMETER VALUES

Parameter	Condition simulated: Normal	Decreased lung compliance	Increased lung damping	Units	Parameter reference
Abdominal compliance	0.1	0.1	0.1	Liters/cm H_2O	*
Chest compliance	0.1	0.1	0.1	Liters/cm H_2O	16
Lung compliance	0.2	0.1	0.2	Liters/cm H_2O	10
Pleural cavity compliance	0.005	0.005	0.005	Liters/cm H_2O	—
Abdominal damping	1.0	1.0	1.0	Cm H_2O/(liters/sec)	*
Chest damping	1.0	1.0	1.0	Cm H_2O/(liters/sec)	12
Lung damping	2.0	2.0	10.0	Cm H_2O/(liters/sec)	10
K_1	3.0	3.0	3.0	Cm H_2O	1
K_2	0.2	0.2	0.2	None	4
K_3	3.0	3.0	3.0	Cm H_2O	—

* From model experimentation.

RESULTS

The accuracy of the simulation can be judged from three computer solutions of the model. The parameters were chosen to model the normal and two abnormal functional states. The two lung disorders are increased airway resistance (larger R_l) and increased lung stiffness (reduced C_l). The pertinent parameter values for all three conditions are shown in Table I.

The simulation results are contained in Figs. 9 to 11. Fig. 9A, 10A, and 11A are plots of system variables vs. time. Figs. 9B, 10B, and 11B are corresponding diagrams with the same variables plotted against a common denominator of lung volume after the manner of Agostoni (2). The pertinent values derived from the curves are summarized in Table II. For each of the three conditions the form and magnitude of the total muscle pressure signal was fixed so that the effects of parameter alteration could be assessed.

Table II presents static and maximum values of system variables depicted graphically in Figs. 9A, 10A, and 11A. Figs. 9B, 10B, and 11B contain the same information but present it in a different manner. The initial values of pressure and volume and the shape of the loops and their angular orientation indicate the condition being simulated. The condition of decreased lung compliance is characterized by a decreased *FRC* and an increased static plural pressure. The pleural pressure loop axis is also rotated counterclockwise as further indication that the lung expands only under greater negative pleural pressures. In the condition of increased lung damping, no change in the *FRC* or static plural pressure is seen, but dynamic effects are demonstrated. The pleural pressure loop encloses a greater

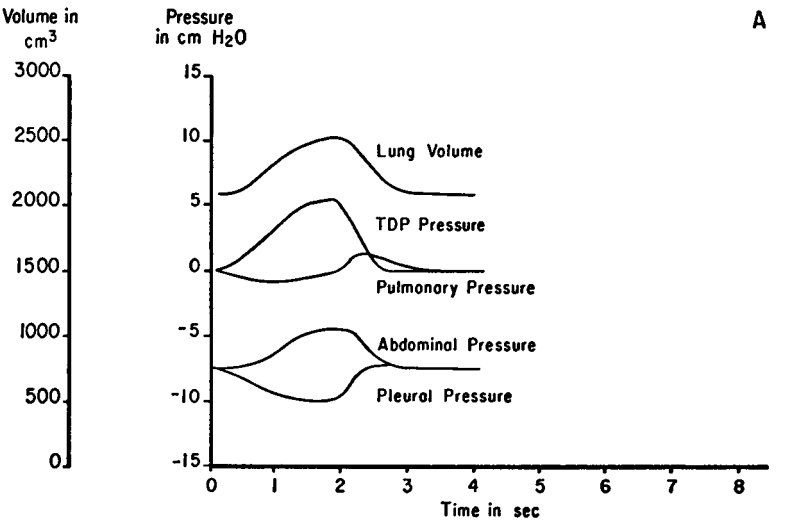

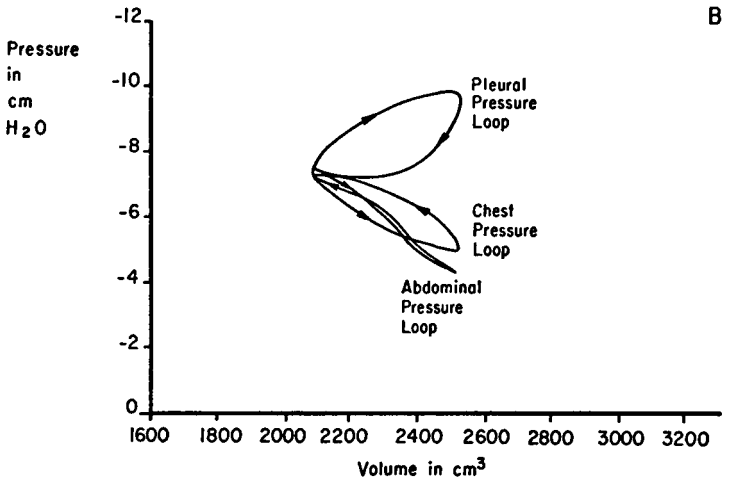

FIGURE 9 In Figs. 9, 10, and 11 simulation results displayed are ink-drawn reproductions of actual computer output data. The results were originally recorded on an IBM 870 autoplotter system operating offline from an IBM 1620 computing system. Simulation results for the normal case: A. system variables vs. time; B. system pressures vs. lung volume.

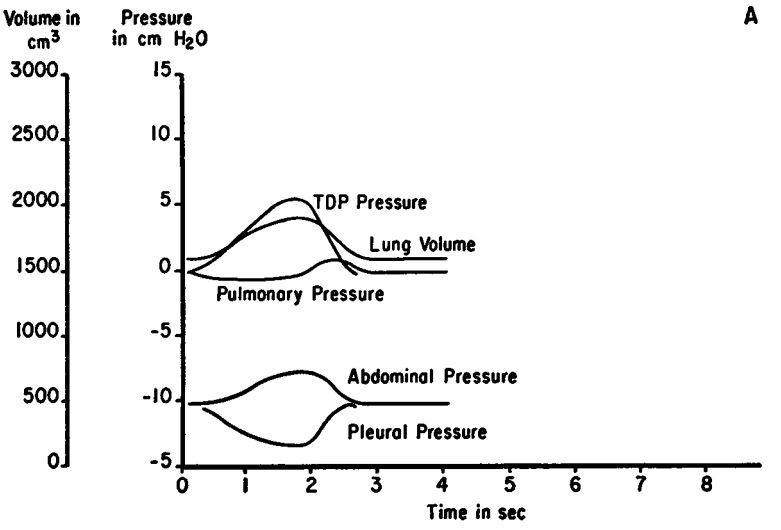

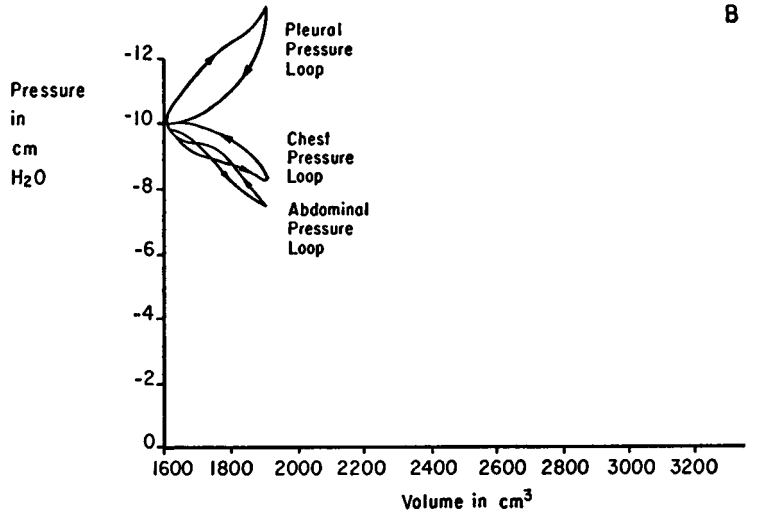

FIGURE 10 Simulation results for the abnormality characterized by decreased lung damping. A. system variables vs. time; B. system pressures vs. lung volume. See also legend Fig. 9.

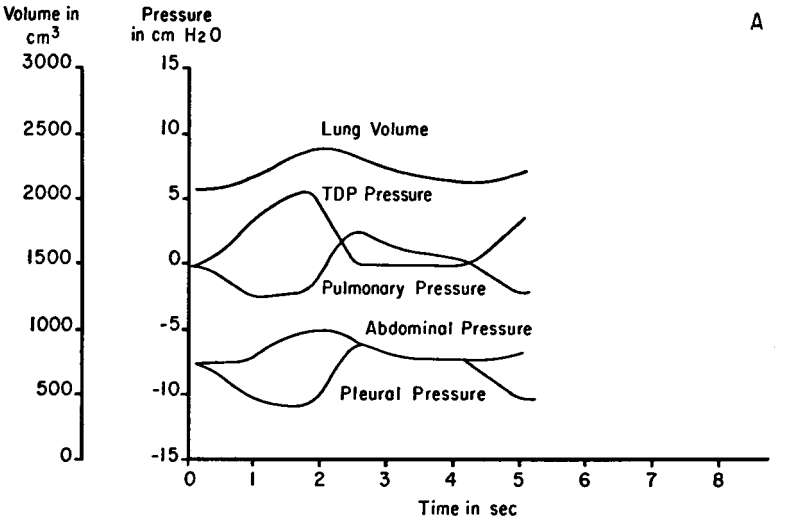

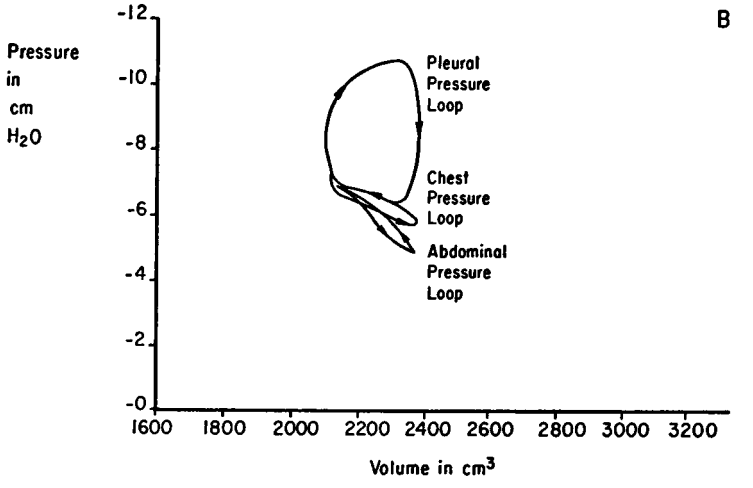

FIGURE 11 Simulation results for the abnormality characterized by increased airway resistance. A. system variables vs. time; B. system pressures vs. lung volume. See also legend Fig. 9.

TABLE II

SIMULATION RESULTS

Parameter	Condition simulated: Normal	Decreased lung compliance	Increased lung damping	Units
Functional reserve capacity	2050	1600	2050	ml
Tidal volume	500	325	375	ml
Static pleural pressure	7.5	10.25	7.5	Cm H_2O
Pleural pressure swing	2.5	3.0	5.0	Cm H_2O
Abdominal pressure swing	3.0	2.5	2.5	Cm H_2O
Maximum transdiaphragmatic pressure	5.5	5.5	5.5	Cm H_2O
Pleural pressure at maximum TDP	2.5	3.0	3.3	Cm H_2O
Abdominal pressure at maximum TDP	3.0	2.5	2.2	Cm H_2O
Maximum inspiratory flow rate	0.5	0.375	0.25	Liters/sec
Maximum expiratory flow rate	0.75	0.625	0.25	Liters/sec
Associated figures	9A, 9B	10A, 10B	11A, 11B	None

area owing to the extra effort required to overcome the added viscous resistance. Similarly, the expiratory phase of the pleural pressure differs, i.e., pleural pressure rapidly increases with little decrease in lung volume.

DISCUSSION

Certain conclusions can be drawn from the data of Table II. (Recall that the driving function is constant for all conditions simulated, since the form of it was derived from the normal case depicted by Agostoni (1).

(*a*) In both abnormal states, an increase in TDP would be required to bring the tidal volume up to normal.

(*b*) Both pulmonary disorders are associated with an increased range of pleural pressure and a reduced variation in abdominal pressure.

(*c*) The maximum inspiratory and expiratory flow rates tend to become the same for the case of increased lung damping. Note that this result is due in part to an assumption made earlier that the lung damping is not variable during the respiratory cycle.

(*d*) The difference between the maximum inspiratory and expiratory flow rates is not greatly affected by a decrease in lung compliance. Their individual magnitudes become smaller, but their difference as read from the graphs (Figs. 9A, 10A, and 11A) is approximately the same.

In the simulation presented here, the time course of the transdiaphragmatic pressure appears to be related to the entire respiratory muscle effort. Figs. 9 to 11 attest to the validity of the system model since the computer results yield waveforms closely resembling functional alterations in ventilation observed in clinical states.

The above model allows observation of the effects of changing a single parameter. In a more general situation with many parameter changes possible, more complex cause-effect relationships can be simulated and individual factors can be separated out and quantified when the corresponding functional relationships are represented mathematically.

The unique characteristic of this investigation lies in its unifying nature. Instead of portraying each parameter or substructure as an entity in itself, this simulation serves to display the individual components in their proper system relationship with one another.

This work was supported in part by the National Institutes of Health Grant HE 07434-01.
Received for publication 8 December 1965.

REFERENCES

1. AGOSTONI, E., *J. Appl. Physiol.*, 1962, **17**, 215.
2. AGOSTONI, E., *J. Appl. Physiol.*, 1961, **16**, 1055.
3. AGOSTONI, E., and RAHN, H., *J. Appl. Physiol.*, 1960, **15**, 1087.
4. AGOSTONI, E. ET AL., *J. Appl. Physiol.*, 1965, **20**, 1179.
5. AGOSTONI, E. ET AL., *J. Appl. Physiol.*, 1965, **20**, 1187.
6. BAYLISS, L. E., and ROBERTSON, G. E., *Quart. J. Exp. Physiol.*, 1939, **29**, 27.
7. CAMPBELL, D., and BROWN, J., *Brit. J. Anaesthesia*, 1963, **35**, 684.
8. COERMANN, R., *Aerospace Med.*, 1960, **31**, 443.
9. DEAN, R. B., and VISSCHER, M. B., *Am. J. Physiol.*, 1941, **134**, 450.
10. RADFORD, E. P., JR., Handbook of Respiration, (D. A. DITTMER and R. M. GREBE, editors), Philadelphia, W. B. Saunders Co., 1958, 133.
11. DUBOIS, A. B., *J. Appl. Physiol.*, 1956, **8**, 587.
12. FERRIS, B. G., JR., MEAD, J., and OPIE, L. H., *J. Appl. Physiol.*, 1964, **19**, 653.
13. FRY, D. L., *Am. J. Med.*, 1960, **29**, 672.
14. MEAD, J., *Physiol. Rev.*, 1961, **41**, 281.
15. MEAD, J., and MILIC-EMILI, J., *in* Handbook of Physiology, (W. O. FENN and H. RAHN, editors), Washington, D. C., American Physiological Society, 1964, sect. 3, **1**, 363.
16. MITTMAN, C. ET AL., *J. Appl. Physiol.* 1965, **20**, 1211.
17. OTIS, A. B., FENN, W. O., and RAHN, H., *J. Appl. Physiol.*, 1950, **2**, 592.
18. RAHN, OTIS, CHADWICK, and FENN, *Am. J. Physiol.*, 1962, **146**, 161.